Taylor & Francis
Taylor & Francis Group

RESEARCH PAPER

OPEN ACCESS ✓ Check for updates

lncRNA CDKN2A-AS1 facilitates tumorigenesis and progression of epithelial ovarian cancer via modulating the SOSTDC1-mediated BMP-SMAD signaling pathway

Qing Zhao*, Dandan Dong*, Huihui Chu, Lu Man, Xinhe Huang, Li Yin, Di Zhao, Lin Mu, Ce Gao, Jianhua Che, and Qian Liu

Department of Obstetrics and Gynecology, The Second Affiliated Hospital of Harbin Medical University, Harbin, China

ABSTRACT

Ovarian cancer (OC) is the fifth most common female malignant tumor and the leading cause of cancer-related death in women worldwide. Epithelial ovarian cancer (EOC) is the predominant type of OC. Investigating the mechanism underlying tumorigenesis and progression of EOC is urgent. Our previous research has shown that long non-coding RNAs (lncRNAs) CDKN2A-AS1 is upregulated in EOC tissues and cells. Furthermore, we have predicted that CDKN2A-AS1 is associated with the bone morphogenetic protein (BMP)-SMAD signaling pathway, which is negatively regulated by the sclerostin domain containing 1 (SOSTDC1). Therefore, we conjecture that the CDKN2A-AS1 regulate BMP-SMAD signaling pathway via interacting with SOSTDC1, which need more investigation. Moreover, the functions of the BMP-SMAD signaling pathway and the SOSTDC1 on EOC are still unclear. Herein, we unearthed that CDKN2A-AS1, BMP2/4/7, SMAD1/5/9 and phosphorylation of SMAD1/5/9 (p-SMAD1/5/9) were upregulated in EOC tissues and cells, whereas SOSTDC1 was downregulated in EOC tissues and cells. We firstly demonstrated that CDKN2A-AS1 bound directly with the SOSTDC1. CDKN2A-AS1 downregulated the expression of SOSTDC1, but upregulated the expression of BMP2/4/7, SMAD1/5/9, and p-SMAD1/5/9. CDKN2A-AS1 promoted the proliferation, migration, invasion of EOC cells and tumor growth in vivo, whereas SOSTDC1 inhibited the proliferation, migration, invasion of EOC cells. Knockdown SOSTDC1 rescued the inhibitory effect of si-lncRNA CDKN2A-AS1 on the EOC cells proliferation, migration and invasion. These results demonstrated that CDKN2A-AS1activated the BMP-SMAD signaling pathway by directly bind with SOSTDC1 to promote EOC tumor growth. CDKN2A-AS1/SOSTDC1 axis may provide a novel therapeutic strategy for EOC treatment.

Introduction

Ovarian cancer (OC) is the most malignant gynecological cancer and the leading cause of cancer-related death in women worldwide [1,2]. Epithelial ovarian cancer (EOC) accounts for approximately 90% of all types of OCs [2]. Lacking obvious symptoms is the predominant reason for the high mortality rate of EOC and the diagnosis of stage III or IV for most patients with EOC [3–5]. Hence, exploring potential diagnostic biomarker and novel efficient therapeutic target is very important for future diagnosis and therapy of EOC.

Among approximately 70% of the transcripts in the human genome that can be transcribed, but only 1–2% can encode proteins, and the rest are non-coding RNAs (ncRNAs) [6]. Of all the ncRNAs, those with lengths of more than 200 nucleotides are named long non-coding RNAs (lncRNAs), accounting for 80–90% of all ncRNAs [7]. Increasing evidence shows that lncRNAs are often imbalanced in tumors and play crucial roles in proliferation, differentiation, invasion and other cell processes [7–12]. Previous studies have shown that lncRNA, such as HOXD-AS1, ANRIL, and GAS5, participatesin the EOC cell proliferation and apoptosis [11–13]. In our previous study, we performed genome-wide lncRNA and mRNA microarray analyses of EOC for the first time, facilitating to further explore roles of candidate lncRNAs in EOC carcinogenesis and subsequent

---

CONTACT Qian Liu ✉ luoluo_liu@sina.com

*These authors contributed equally to this work.
ⓘ Supplemental data for this article can be accessed here

progression [14]. The expression of lncRNA CDKN2A-AS1 was upregulated in EOC tissues and cells [5,14]. Nevertheless, the role of CDKN2A-AS1 in EOC and the underlying mechanism have not been studied sufficiently, which need to be further investigated. Many signaling pathways are highly correlated with the progression and recurrence of OC [14–16]. We conducted Kyoto encyclopedia of genes and genomes (KEGG) pathways analysis and found that CDKN2A-AS1 was primarily involved in bone morphogenetic protein (BMP)-SMAD signaling pathway, transcriptional mis-regulation in cancer, MAPK signaling pathway significantly (Figure 1c). BMP ligands are overexpressed in OC, which is correlated with poor progression-free survival (PFS) of OC [15,17]. As a negative regulator of the BMP-SMAD signaling pathway, sclerostin domain containing 1 (SOSTDC1) has been shown to be associated with the development and progression of a variety of cancers, including breast, stomach, kidney and thyroid cancers [18–22]. In light of the above-mentioned results and literature, we presumed that CDKN2A and SOSTDC1 interacted with each other and even worked together in the progression of EOC via BMP signaling pathway, which needed more evidence.

Then, we investigated whether lncRNA CDKN2A-AS1 is dysregulated in EOC and how dysregulated CDKN2A-AS1 participates in the pathological process of EOC. We detected the differential expression of CDKN2A-AS1 and SOSTDC1 in 15 pairs of EOC tissues and normal tissues. Furthermore, RNA fluorescent in situ hybridization (RNA-FISH) assay, pull-down assay, western blot assay and dual-luciferase reporter assay were implemented to verify the interaction between CDKN2A-AS1 and SOSTDC1. Next, we detected the expression level of SOSTDC1,
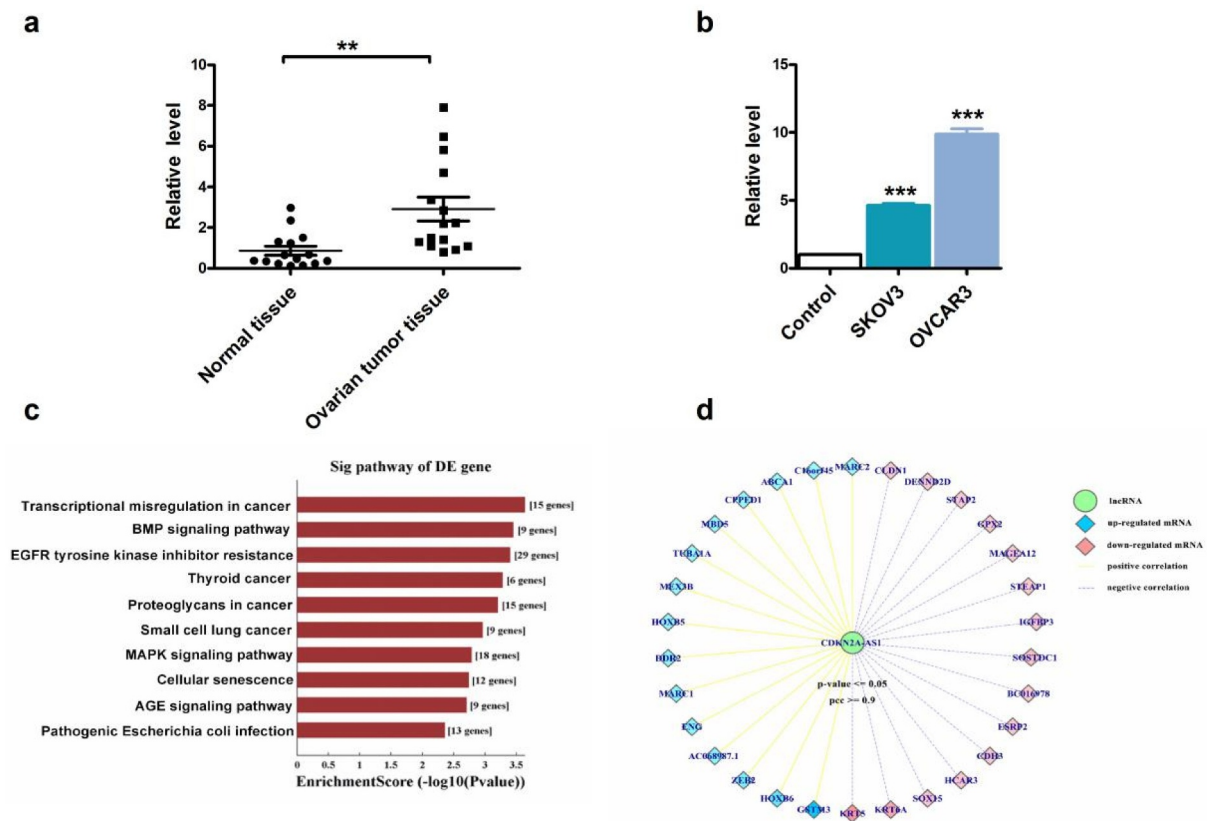

Figure 1. Identification and characterization of CDKN2A-AS1 in EOC. (a) Relative gene expression levels of CDKN2A-AS1 in 15 paired ovarian tumor tissues and normal ovary tissue samples. (b) Relative expression of CDKN2A-AS1 in IOSE80,SKOV3, and OVCAR3 cell lines. (c) KEGG pathway analysis of CDKN2A-AS1. (d) CDKN2A-AS1 CNC analysis results. The lines between the red and blue nodes represent interactions between CDKN2A-AS1 and proteins. Solid lines indicate positive correlations, whereas a dashed line indicates a negative correlation. *$p < 0.05$, **$p < 0.01$, ***$p < 0.001$ vs normal tissue (control).

BMP2/4/7, SMAD1/5/9, p-SMAD1/5/9, matrix metalloproteinase-2 (MMP2) after overexpression, or inhibition of CDKN2A-AS1 in the SKOV3 and OVCAR3 cell lines. Our results demonstrated that CDKN2A-AS1 promoted proliferation and invasion of EOC cells by targeting SOSTDC1 and activating the BMP-SMAD signaling pathway. This study provided novel insights into the crucial involvement of the lncRNA CDKN2A-AS1 in the tumorigenesis and progression of EOC.

Materials and methods

Patients and ovary tissue specimens

From September 2016 to December 2017, ovary tissue specimens (ovarian tumors and normal tissues) were obtained from 15 patients with EOC who underwent surgery at the Second Affiliated Hospital of Harbin Medical University (Harbin, China). The research was approved by the Ethics and Scientific Committees of Harbin Medical University.

Cell culture

The two EOC cell lines (SKOV3 and OVCAR3) were cultured at 37°C in 5% CO_2 in RPMI-1640 medium (HyClone, Logan, UT, USA) containing 10% and 15% fetal bovine serum (FBS) (HyClone; GE Healthcare Life Sciences). The normal ovarian epithelial IOSE80 cell lines were cultured in Dulbecco's modified Eagle medium (HyClone, Logan, UT, USA) supplemented with 10% FBS (HyClone; GE Healthcare Life Sciences). For the transfection procedure, SKOV3 and OVCAR3 cells were starved in serum-free RPMI-1640 medium for 24 h and then transiently transfected with si-lncRNA (CDKN2A-AS1 siRNA) or nonsense control of si-lncRNA (si-NC) (RiboBio Co., Ltd., Guangzhou, China). X-treme GENE siRNA transfection reagent (cat. no. 04476093001; Roche Diagnostics GmbH, Mannheim, Germany) was used for transfection according to the manufacturer's instructions. pcDNA-lncRNA (CDKN2A-AS1), nonsense control of pcDNA-lncRNA (pcDNA-NC), pcDNA-SOSTDC1, si-SOSTDC1 (SOSTDC1 siRNA) or control plasmids were purchased from Integrated Biotech Solutions Co., Ltd.

(Shanghai, China) and were transfected into cells using Lipofectamine 2000 (Invitrogen, Carlsbad, CA, USA). After transfection for 48 h, cells were harvested. The information about siRNA is shown in Table 1.

Quantitative real-time PCR (qRT-PCR) assay

SOSTDC1 mRNA levels were determined by qRT-PCR assay. Briefly, total RNA was harvested from tissues using 1 ml of Trizol reagent (Invitrogen, Carlsbad, CA, USA) according to the manufacturer's protocols. cDNA synthesis was performed using the High Capacity cDNA Reverse Transcription Kit in the light of the manufacturer's instructions. The SYBR Green PCR Master Mix Kit (cat. no. 4309155; Applied Biosystems) was used to quantify the relative mRNA levels of SOSTDC1. GAPDH was chosen as an internal control. The sequences of the primers are as follows:

SOSTDC1 forward, 5'-ACCTGCTTCTTAGAGGGCCTGGAC-3', and reverse, 5'- GACTCGTTGTGCTGCCGGGT-3',GAPDH forward, 5'-AAGAAGGTGGTGAAGCAGGC-3',and reverse, 5'-TCCACCACCCAGTTGCTGTA-3';CDKN2A-AS1 forward, 5'-GAGGCCTGGTGAGCAAAATA-3',and reverse, 5'-AAAGCCGTGTCTCAAGATCG-3'

Western blotting assay (WB)

Homogenized specimens or cells were grounded in 500 μlRIPA buffer containing protease and phosphatase inhibitors, followed by centrifugation at 13,500 rpm for 25 min. The protein concentration in the supernatant was tested by the BCA Protein Assay (Beyotime, Shanghai, China). A 12% SDS-

Table 1. The information about siRNA is shown below.

Name	Sequence:(5'to3')	Size
CDKN2A-AS1-1	CGAUGAAAUUGUUGUAAUAdTdT	21
CDKN2A-AS1-1_AS	UAUUACAACAAUUUCAUCGdTdT	21
CDKN2A-AS1-2	CAAUAAAUGUUGACAAUAAdTdT	21
CDKN2A-AS1-2_AS	UUAUUGUCAACAUUUAUUGdTdT	21
CDKN2A-AS1-3	GCUCAAAUAAUGUUGACAAdTdT	21
CDKN2A-AS1-3_AS	UUGUCAACAUUUAUUGAGCdTdT	21
SOSTDC1	CAGUCACAACUUUGAGAGCdTdT	21
SOSTDC1_AS	GCUCUCAAAGUUGUGACUGdTdT	21

PAGE gel electrophoresis was used for fractionating total proteins, and then the proteins were transferred onto nitrocellulose membranes. The membranes were blocked in PBS solution containing 5% defatted milk for 2 h at room temperature following incubation at 4°C overnight with primary antibodies against SOSTDC1 (1:1000) (Cloud-Clone Corp., Inc., Wuhan, China), BMP2 (1:500) (Wanleibio, Inc., Shenyang, China), BMP4 (1:500) (Wanleibio, Inc., Shenyang, China), BMP7 (1:1000) (Wanleibio, Inc., Shenyang, China), SMAD1/5/9 (1:1000) (Cell Signaling Technology, Inc., Shanghai, China), or p-SMAD1/5/9 (1:1000) (Cell Signaling Technology, Inc., Shanghai, China), MMP2 (1:2000) (ab235167). GAPDH (1:1000) (Wanleibio, Inc., Shenyang, China) was used as an internal control. Matched secondary antibody (1:10,000) (LI-COR, Lincoln, NE, USA) was incubated for 1 h at room temperature. Protein expression was scanned and quantified by the Odyssey Infrared Imaging System (LI-COR Biosciences, Lincoln, USA).

Cell proliferation assay

The Cell Counting Kit-8 (CCK-8) (Dojindo, Kumamoto, Japan) was used to detect cell proliferation. SKOV3 and OVCAR3 cells were transfected with specific reagents for 24 h and then plated in a 96-well plate and cultivated for 24 h. Next, 10% CCK-8 solution was added to the cell culture medium for a 1 h incubation until color change. Optical density values were determined by a microplate reader, and proliferation rates were then calculated.

Cell migration and invasion assay

Cells were seeded in six-well plates with a complete medium to analyze wound healing. After 24 h, the cell monolayer was scratched with a plastic pipette tip. Then, the cells were rinsed with PBS and cultured with complete RPMI-1640 for 24 h. The wound closure was observed and photographed under a microscope. For the transwell migration assay, 8 μm pore size polycarbonate membrane 24-well Transwell was used. For the invasion assay, 8 μm pore size polycarbonate membrane 24-well Transwell coated with a Matrigel (BD Bioscience) was used. Twenty-four hours after the transfection, cells in serum-free RPMI-1640 medium were plated into the upper chamber, while 10% FBS RPMI-1640 medium was added to the lower chamber. After 24 h of incubation, the cells that migrated and invaded into the lower chamber through the membrane were fixed with 100% methanol for 15 min and stained with 0.1% crystal violet for 20 min. Images of the cells were photographed with a microscope.

Immunofluorescence staining assay

For immunofluorescence staining, SKOV3 and OVCAR3 cells were fixed with 4% paraformaldehyde in PBS. Then, the cells were incubated with blocking solution (5% BSA and 0.1% Triton-X in PBS) for 2 h at room temperature and subsequently blocked with 5% BSA dissolved in PBS for 2 h. Primary antibodies against SOSTDC1 (1:200) (Cloud-Clone Corp., Inc., Wuhan, China) and KI-67 (1:100) (Wanleibio, Inc., Shenyang, China) were added overnight at 4°C, followed by incubation with the matched secondary antibody (1:500) (cat. no. A-11032; Invitrogen, Carlsbad, CA, USA) for 1 h at 37°C. The nuclei were stained with DAPI (1:100) for 20 min at room temperature (Beyotime, Shanghai, China). Finally, the cells were examined and analyzed by laser confocal microscopy (FV300, Olympus, Japan).

RNA fluorescent in situ hybridization (RNA-FISH)

The CDKN2A-AS1 probe was designed and produced by RiboBio (Guangzhou, China). SKOV3 cells were cultured in 24-well plates overnight and then fixed with 4% paraformaldehyde for 10 min before treatment with 0.5% Triton X-100 for 10 min. Then, cells were incubated in prehybridization solution, next hybridization solution containing the probe was added and incubated overnight at 37°C. After washing by PBS, 6-diamidino-2-phenySlindole (DAPI) was used to sign the nucleus. CDKN2A-AS1 was observed under a fluorescence microscope.

RNA-protein pull-down assay

For in vitro RNA pull-down, 5 ml of cell lysates from SKOV3 cells was incubated with 1 mg biotin-16-UTP-labeled CDKN2A-AS1 in immunoprecipitation buffer for 30 min at 25°C. After the addition of 5 ml MyOne Streptavidin T1 Dynabeads (Invitrogen, Inc., CA, USA), the mixture was incubated for an additional 30 min and subjected to five wash cycles with a 500 ml IPB buffer for 5 min each. After the final wash, magnetic beads were resuspended in a 12 ml protein-loading buffer, and RNA-bound proteins were separated by SDS-PAGE and detected with anti-SOSTDC1 (Cloud-Clone Corp., Inc., Wuhan, China) by WB.

Bioinformatics prediction and Dual-Luciferase reporter assay

A web-based program known as Freiburg RNA tools program (http://rna.informatik.uni-freiburg.de) was used to predict the target genes of lncRNA CDKN2A-AS1 and SOSTDC1. Their conserved sites matched the seed region.To do the dual-luciferase reporter assay, the wildtype or mutant SODTDC1in psiCHECKvector was co-transfected with CDKN2A-AS1, si-CDKN2A-AS1, pcDNA3.1 or siRNA NC into HEK293T cells using lipofecta-mine 2000 transfection reagent (Thermo Fisher Scientific). The dual-luciferase reporter assay was performed 48 h post-transfection using dual-luciferase assay system (Promega). The luciferase activity of each sample was normalized to the Renilla luciferase activity.

Nude mouse and xenograft transplantation

Athymic female nude mice were obtained from the animal center of Harbin Medical University at 3 weeks of age and raised until 5 weeks old. A total of 3×10^6 OVCAR3 cells transfected with lncRNA or sh-lncRNA or NC were subcutaneously injected into the upper back of each mouse (n = 3 mice/group). Mice were killed after 40 days. The weight and size of the tumors were measured. The study protocol was approved by the Animal Ethic Committees of Harbin Medical University.

Pathway analysis

We performed a path analysis of the differentially expressed mRNAs to identify rich biological pathways that are based on P < 0.05 by using the latest KEGG database (http://www.genome.jp/kegg).

CNC network analysis

Calculate the correlation coefficient between the normalized data of the selected LncRNA and all Genes in the mRNA list, and select records that meet abs (pcc)≥ 0.9, p-value ≤ 0.05, and fdr≤ 1 Draw with Cytoscape v2.8.3 tools.

Complex structure prediction

The three-dimensional structures of CDKN2A-AS1 and SOSTDC1 were simulated by SYBYL and PYMOL software.

Statistical analysis

Group data was analyzed as the mean ± standard error of the mean (SEM). Significant differences were analyzed by Student's t-test for two groups or one-way analysis of variance (ANOVA) test for more than two groups. Bonferroni's multiple-comparison test was performed for comparison of intergroup differences. Only p < 0.05 was considered statistically significant. Data were analyzed by applying GraphPad Prism 5.0 software (GraphPad Software, Inc., La Jolla, CA, USA).

Results

CDKN2A-AS1 is dysregulated in EOC

Based on the previous microarray results of the lncRNAs, we identified four with the most significant differential expression between OC and normal ovary cells (CDKN2A-AS1, LINC00184, LINC-PINT, and LOC100133669) [14]. To further investigate the function of CDKN2A in EOC, we determined the expression level of CDKN2A-AS1 in 15 pairs of ovary biopsy samples from EOC patients, three cell lines (IOSE80, SKOV3, OVCAR3). The expression levels of CDKN2A-AS1 in EOC tissues and EOC cells (SKOV3 and

OVCAR3) were evidently higher than that in normal ovary tissues and normal ovarian epithelial IOSE80 cells, respectively (Figure 1a,b). Moreover, to further explore the biological function of CDKN2A-AS1 in EOC, KEGG pathways analysis showed that CDKN2A-AS1 was primarily associated with BMP-SMAD signaling pathway, transcriptional misregulation in cancer, MAPK signaling pathway significantly (Figure 1c). CNC network was constructed to identify mRNAs associating with CDKN2A-AS1. We selected 30 target mRNAs for CDKN2A-AS1, which play important roles in cancer progression (Figure 1d).

CDKN2A-AS1 regulates BMP signaling by directly binding with SOSTDC1

To investigate the functions of SOSTDC1 and the BMP-SMAD signaling pathway in EOC, the expression level of SOSTDC1 in 15 pairs of EOC tissues and normal ovarian tissues samples were evaluated by qRT-PCR. Compared with normal tissues, mRNA levels and protein expression levels of SOSTDC1 in EOC tissues were downregulated (Figure 2a,b). Numerous studies have indicated that SOSTDC1 inhibits the BMP-SMAD signaling pathway by binding BMP proteins, including
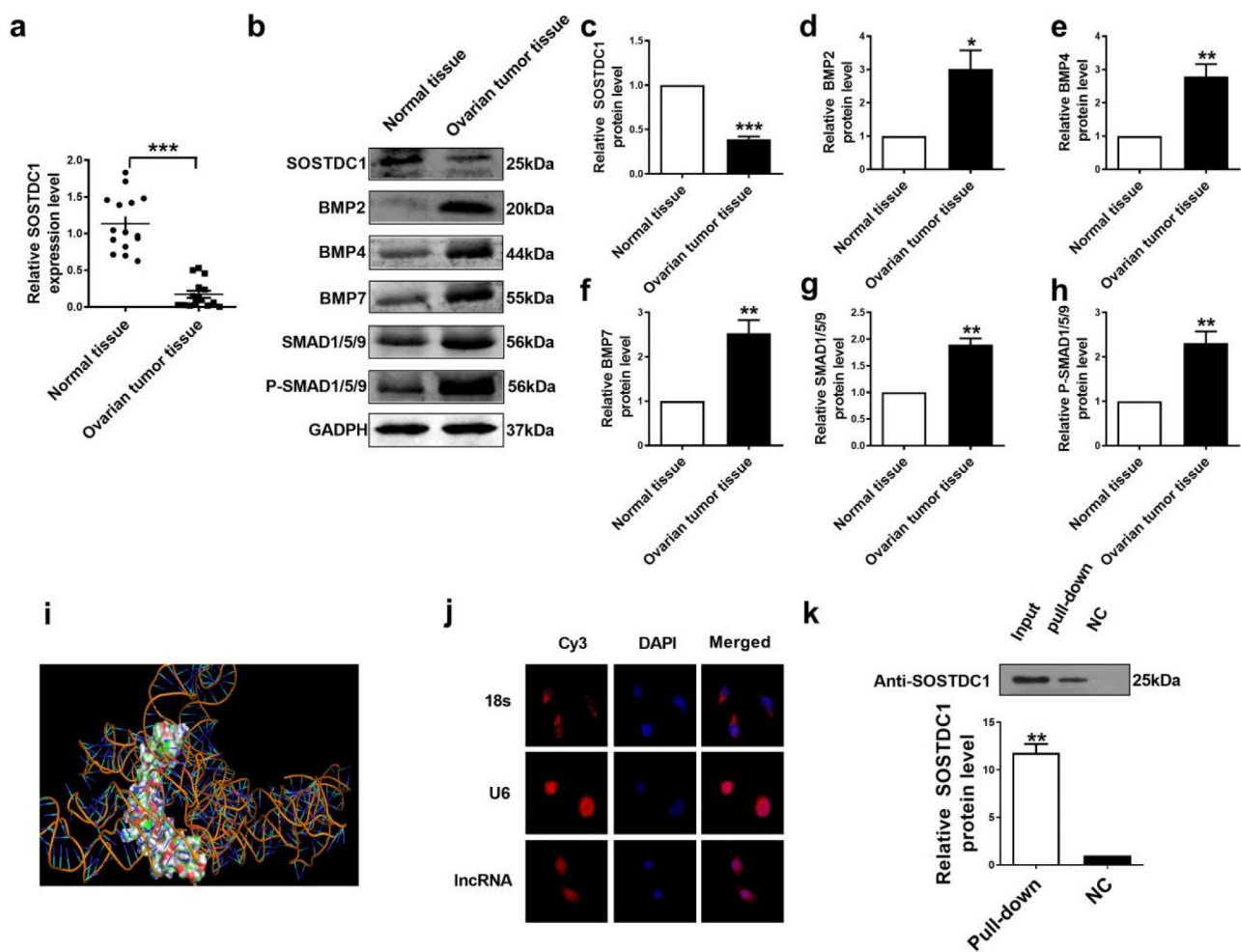

Figure 2. SOSTDC1, BMP-2, −4, and −7 and downstream SMAD proteins were deregulated in ovarian tumor tissues. (a) Relative gene expression levels of SOSTDC1 in 15 paired ovarian tumor tissues and normal ovary tissue samples. (b) Representative western blotting bands of the proteins. (c-h) Relative protein expression levels of SOSTDC1, BMP-2, BMP-4, BMP-7, SMAD1/5/9, and p-SMAD1/5/9. (i) The combination of CDKN2A-AS1 and SOSCDT1 three-dimensional structure was simulated by SYBYL and PYMOL software. (j) Representative images of FISH assays showing the expression of CDKN2A-AS1 in SKOV3 cells. (k) Pull-down of SOSTDC1 by CDKN2A-AS1 in SKOV3 cells. NC: normal control. $*p < 0.05$, $**p < 0.01$, $***p < 0.001$ vs normal tissue.

BMP-2, −4, 6 and −7 [19,21,22]. The interaction network of the protein SOSTDC1 and BMP1, BMP4, BMP6, and BMP7 was searched in the STRING. The combined-scores were shown in Fig S2. The combined-score between SOSTDC1 and BMP6 is 0.603, which is lower than those of SOSTDC1 and BMP2, BMP4, and BMP7. Therefore, we chose to detect the expression of BMP2, BMP4, and BMP7. The protein expression levels of BMP-2, −4, and −7 and the expression of phosphorylation levels of SMAD1/5/9 and SMAD1/5/9 were obviously increased in EOC tissues compared with those in normal ovarian tissues (Figure 2b–h). These results further validated the negatively regulated role of SOSTDC1 in the BMP-SMAD signaling pathway in EOC. For analysis of the association between the lncRNA CDKN2A-AS1 and SOSTDC1, the prediction tool RPISeq (RNA-Protein Interaction Prediction, http://pridb.gdcb.iastate.edu/RPISeq/) was applied. A high probability of lncRNA–protein interaction existed between them (a probability of 0.85 using the random forest classifier and a probability of 0.91 using the support vector machine classifier). The combination of CDKN2A-AS1 and SOSTDC1 three-dimensional structure was simulated by SYBYL and PYMOL software, and we found that strongly connected between CDKN2A-AS1 and SOSTDC1 (Figure 2i). Analysis of RNA isolated from the cytoplasmic and nuclear compartments of SKOV3 cells and cellular FISH experiments showed that CDKN2A-AS1 was present both in the cytoplasm and cell nucleus (Figure 2j). Pull-down assay was used to prove whether CDKN2A-AS1 interacts with SOSTDC1. We detected the protein SOSTDC1 in the pcDNA lncRNA (CDKN2A-AS1) group, but did not detect the protein SOSTDC1 in the NC group. The level of SOSTDC1 in the CDKN2A-AS1 group was obviously higher than that in the NC group, which is statistically significant (p < 001) (Figure 2k). The results showed that CDKN2A-AS1 interacted with the SOSTDC1.

To further prove direct binding between lncRNA CDKN2A-AS1 and SOSTDC1, the bioinformatic analysis and dual-luciferase reporter assay were performed. Bioinformatics analysis predicted that there is one binding site between lncRNA CDKN2A-DT and SOSTDC1 (Figure 3a). The sequences of lncRNA CDKN2A-AS1, SOSTDC1 and SOSTDC1-Mut are shown in Figure 3b. The Figure 3c,d showed that lncRNA CDKN2A-AS1 obviously reduced the luciferase activity of psiCHECK-SOSTDC1, but not psiCHECK-SOSTDC1-Mut (p < 0.01). The relative luciferase activity was calculated (Figure 3e). The relative luciferase activity of the group co-transfected with lncRNA CDKN2A-AS1and psiCHECK-SOSTDC1 was 55% of that of the control group (p < 0.01). The relative luciferase activity of the group co-transfected with lncRNA CDKN2A-AS1 and psiCHECK-SOSTDC1-Mut has no different change compared with the control group. The results indicated that lncRNA CDKN2A-AS1 indeed directly bound with SOSTDC1 and there is only one binding site between lncRNA CDKN2A-AS1 and SOSTDC1.

Knockdown of CDKN2A-AS1 inhibits ovarian cancer cell proliferation and migration

The si-lncRNA against CDKN2A-AS1 was successfully transfected into OVCAR3 and SKOV3 cells. Immunofluorescence staining showed that cell fluorescence of si-lncRNA CDKN2A-AS1 group was increased obviously compared with the control group and NC group (Figure 4a,b). The expression level of SOSTDC1 in si-lncRNA CDKN2A-AS1 group was higher than that in control group and NC group (Figure 4a,b). KI67 staining showed that the cell fluorescence and the expression of KI67 in si-lncRNA CDKN2A-AS1 group were decreased obviously compared with the control group and NC group (Figure 4c,d), which indicated that inhibition of CDKN2A-AS1 suppressed the proliferation of the OVCAR3 and SKOV3 cells. CCK-8 analysis (Figure 4e) further confirmed that inhibition of CDKN2A-AS1 suppressed the proliferation of the OVCAR3 and SKOV3 cells. Transwell assays indicated that the invasive ability of both cells was obviously decreased with si-lncRNA-mediated downregulation of CDKN2A-AS1 (Figure 4f,g). In addition, the cell scratch test revealed that transfection of si-lncRNA resulted in a decline in the migration capacity of the two cells (Figure 4h,i).
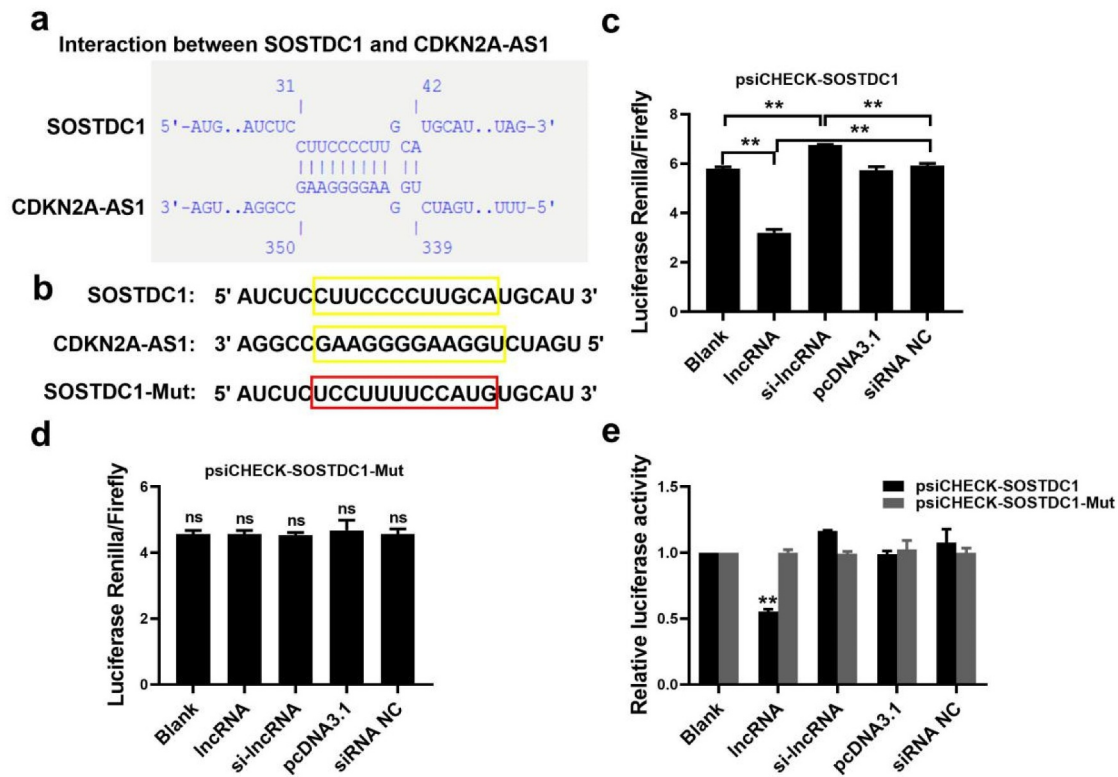
Figure 3. CDKN2A-AS1 directly target SOSTDC1. (a) Bioinformatics analysis showed the predicted CDKN2A-AS1 binding sites in SOSTDC1. (b)The sequences of the SOSTDC1, SOSTDC1-Mutant and CDKN2A-AS1. (c) The dual-luciferase reporter assay was performed to determine luciferase activity in cell co-transfected withpsiCHECK-SOSTDC1 and CDKN2A-AS1,si-CDKN2A-AS1, pcDNA3.1 or siRNA NC. (d) The dual-luciferase reporter assay was performed to determine luciferase activity in cell co-transfected with psiCHECK-SOSTDC1-Mut and CDKN2A-AS1,si-CDKN2A-AS1, pcDNA3.1 or siRNA NC. (e) The relative luciferase activity was calculated.**$p < 0.01$ vs control.

Effects of transfection of siRNA against CDKN2A-AS1 on the BMP-SMAD signaling

To demonstrate a downstream regulatory target of CDKN2A-AS1, the expression levels of SOSTDC1 in both OVCAR3 and SKOV3 cells were investigated. The protein expression level of SOSTDC1 was obviously increased after CDKN2A-AS1 suppression in both OVCAR3 and SKOV3 cells by western blotting assay (Figure 5a–c). Whereas the protein expression levels of BMP-2, −4, and −7 and the expression of phosphorylation levels of SMAD1/5/9 (p-SMAD1/5/9) and SMAD1/5/9 were obviously decreased in both cell lines (Figure 5d–h)

Overexpression of CDKN2A-AS1 promotes ovarian cancer cell proliferation and migration

The recombinant plasmid pcDNA-CDKN2A-AS1 was successfully transfected into OVCAR3 and SKOV3 cells. Immunofluorescence staining showed that cell fluorescence of pcDNA-lncRNA CDKN2A-AS1 group was decreased obviously compared with the control group and NC group (Figure 4a,b). The expression level of SOSTDC1 in pcDNA CDKN2A-AS1 group was lower than that in control group and NC group (Figure 6a,b). KI67 staining (Figure 6c,d) and the CCK-8 assay (Figure 6e) suggested that upregulation of CDKN2A-AS1 enhanced the propagation of both OVCAR3 and SKOV3 cells. Transwell assays demonstrated that
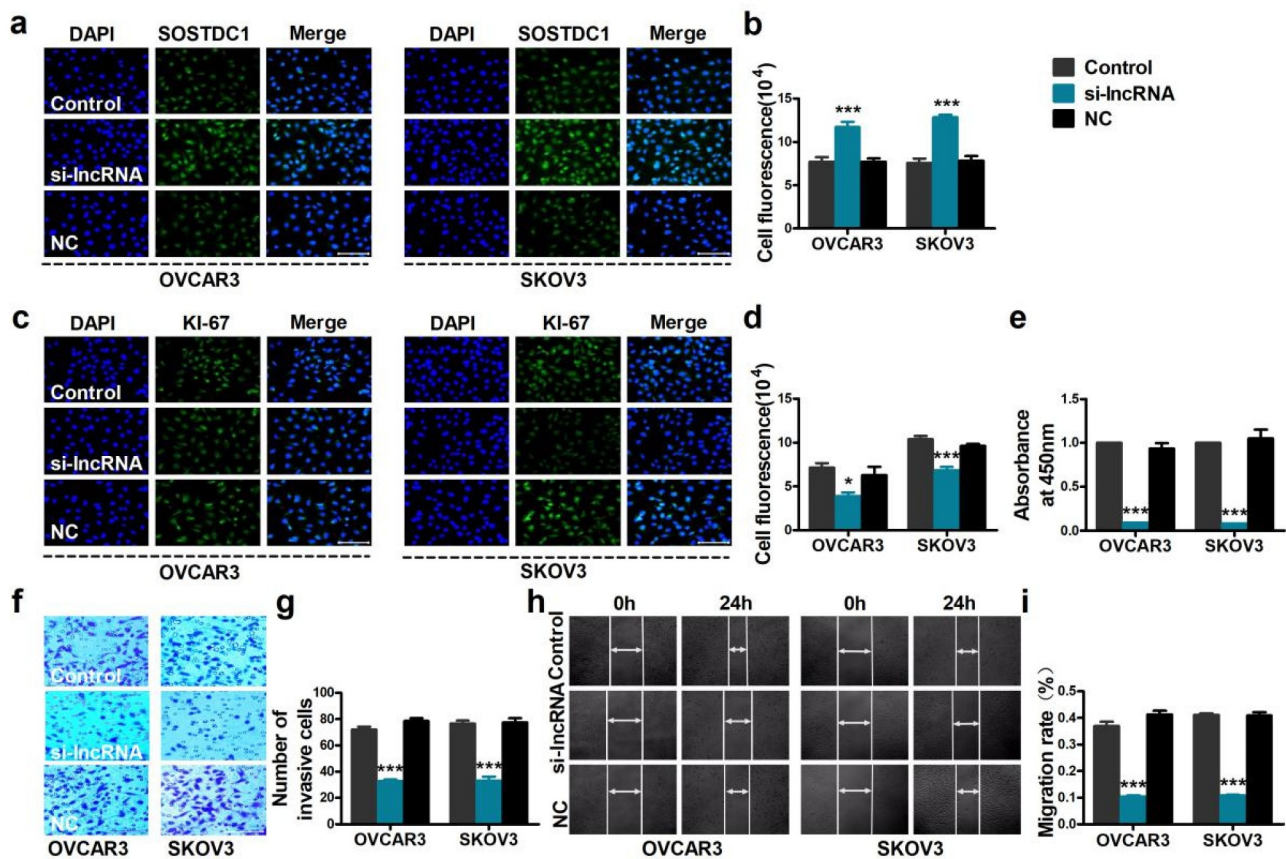
Figure 4. Proliferation and migration of OVCAR3 cells and SKOV3 cells were inhibited by knockdown of CDKN2A-AS1. (a) Representative images of immunofluorescence staining showing expression of SOSTDC1 in OVCAR3 and SKOV3 cells. Scale bar indicates 50 μm. (b) The fluorescence intensity of SOSTDC1 was counted. (c) Representative images of immunofluorescence staining showing expression of KI67 in OVCAR3 and SKOV3 cells. Scale bar indicates 50 μm. (d) The fluorescence intensity of KI67 was counted. (e) Results of the CCK-8 assay in OVCAR3 cells and SKOV3 cells. (f and g) Effect of si-CDKN2A-AS1 downregulation on the invasion of OVCAR3 cells and SKOV3 cells was assessed by the transwell assay. Scale bar indicates 100 μm. (h and i) Wound healing assay showed that si-CDKN2A-AS1 caused a slower closing of scratch wounds. **$p < 0.01$, ***$p < 0.001$ vs. control.

overexpression of CDKN2A-AS1 markedly facilitated cell viability in both OVCAR3 and SKOV3 cells (Figure 6f,g). Additionally, cell migration of both OVCAR3 and SKOV3 cells was enhanced by transfection of pcDNA-CDKN2A-AS1 (Figure 6h,i).

Effects of transfection of pcDNA CDKN2A-AS1 on the BMP-SMAD signaling

To reverse validate the function of CDKN2A-AS1 in EOC development, we transfected SKOV3 and OVCAR3 cells with pcDNA targeting CDKN2A-AS1. The protein expression level of SOSTDC1 was obviously decreased after CDKN2A-AS1 overexpression in both OVCAR3 and SKOV3 cells (Figure 7a–c). Consistently, the protein expression levels of BMP-2, −4, and −7 and the expression of

phosphorylation levels of SMAD1/5/9 (p-SMAD1/5/9) and SMAD1/5/9 were obviously increased in both cell lines (Figure 7d–h).

Inhibiting SOSTDC1 can rescue the decrease of ovarian cancer cell proliferation and migration induced by suppressing CDKN2A-AS1

Compared with the control group, downregulation of the CDKN2A-AS1 (si-lncRNA group) or overexpression of the SOSTDC1 (SOSTDC1 group) decreased the proliferation and migration of the ovarian cells. Compared with the si-lncRNA group or SOSTDC1 group, the proliferation and migration of ovarian cells were further reduced by co-transfecting si-lncRNA and SOSTDC1 (si-lncRNA/SOSTDC1 group). The proliferation and migration of ovarian cells in si-lncRNA/si-SOSTDC1
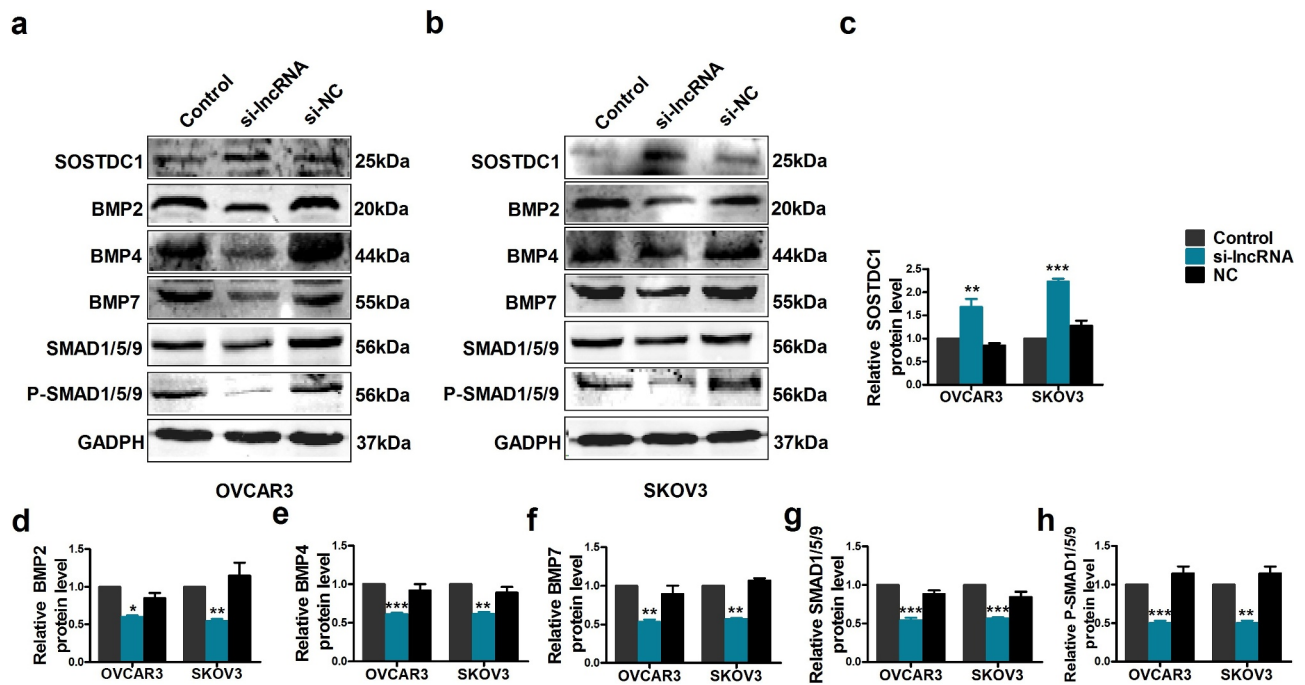
Figure 5. Effects of transfection of siRNA against CDKN2A-AS1 on the BMP-SMAD signaling pathway in SKOV3 and OVCAR3 cells. (a) Representative western blotting bands of proteins in OVCAR3 cells. (b) Representative western blotting bands of proteins in SKOV3 cells. Results of western blotting of SOSTDC1 (c), BMP2 (d), BMP4 (e), BMP7 (f), SMAD1/5/9 (g), and p-SMAD1/5/9 (h) in OVCAR3 cells and SKOV3 cells. *$p < 0.05$, **$p < 0.01$, ***$p < 0.001$ vs control.

group were higher than those in si-lncRNA group, SOSTDC1 group, si-lncRNA/SOSTDC1 group, while lower than those in the control group. The above results indicated that the negative relationship between CDKN2A-AS1 and SOSTDC1. Downregulation of the SOSTDC1 (si-SOSTDC1) obviously rescued the inhibitory effect of si-lncRNA CDKN2A-AS1 on the ovarian proliferation and migration. To detect the relationship between SOSTDC1 and BMP-SMAD, the protein expression level of the BMP2, SMAD and p-SMAD in ovarian cells transfected with SOSTDC1 or siRNA against SOSTDC1were determined by WB (Figure 8d,e). Compared with the control group, overexpression of SOSTDC1 decreased the expression level of the BMP2 and SMAD (SOSTDC1 group and si-lncRNA /SOSTDC1 group), which demonstrated the negative relationship between SOSTDC1 and BMP-SMAD signaling pathway.

The expression of MMP2 in ovarian cells was determined. MMP2 played important role in promoting the process of cancer cell invasion. Downregulating the lncRNA CDKN2A-AS1 (si-

lncRNA group) decreased the expression of MMP2 (Figure 8d,e) and the invasion ability of ovarian cells (Figure 4f,g), which is consistent with previous studies.

lncRNA CDKN2A-AS1 promoted tumor progression

On the basis of the above-mentioned results, we researched the function of lncRNA in vivo xenograft. Compared with the control group, the tumor volume and weight in lncRNA group were obviously increased, whereas the tumor volume and weight in si-lncRNA group were reduced (Figure 9a–c). Overexpressing the lncRNA CDKN2A-AS1 promoted the tumor growth, while knockdown of the lncRNA CDKN2A-AS1 suppressed the tumor growth (Figure 9a–c).

Discussion

EOC is the most aggressive subtype of OC [2]. High recurrence and mortality rates are obvious characteristics when compared to other subtypes
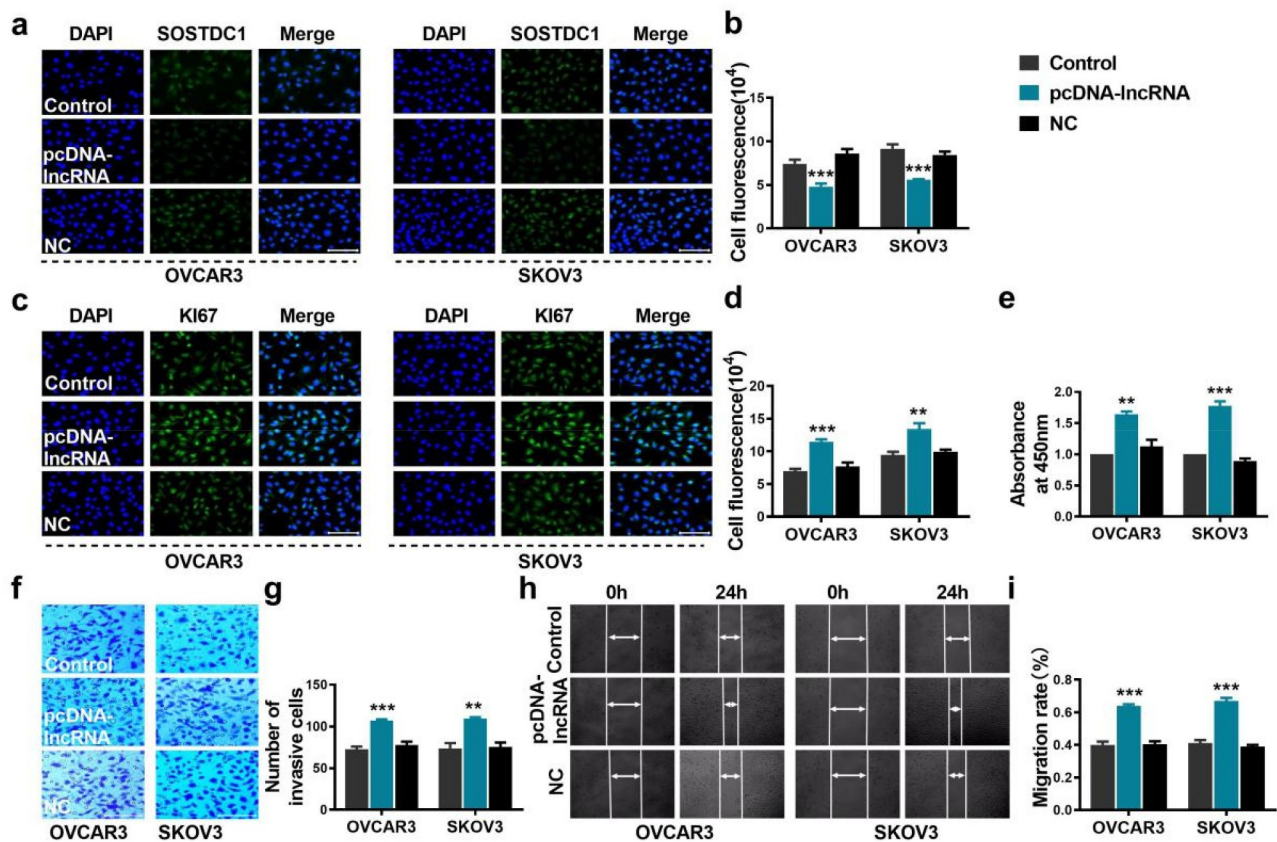
Figure 6. Effects of overexpression of CDKN2A-AS1 on the proliferation and migration of OVCAR3 cells and SKOV3 cells. (a) Representative images of immunofluorescence staining showing the expression of SOSTDC1 in OVCAR3 and SKOV3 cells. Scale bar indicates 50 μm. (b) The fluorescence intensity of SOSTDC1 was counted. (c) Representative images of immunofluorescence staining showing the expression of KI67 in OVCAR3 and SKOV3 cells. Scale bar indicates 50 μm. (d) The fluorescence intensity of KI67 was counted. (e) Results of the CCK-8 assay in OVCAR3 cells and SKOV3 cells. (f and g) Effect of pcDNA-CDKN2A-AS1 upregulation on the invasion of OVCAR3 cells and SKOV3 cells was assessed by the transwell assay. Scale bar indicates 100 μm. (h and i) Wound healing assay showed that pcDNA-CDKN2A-AS1 caused a faster closing of scratch wounds. $**p < 0.01$, $***p < 0.001$ vs control.

of OC [2,13,23]. Most patients with EOC have intraperitoneal dissemination at the time of diagnosis, contributing to an average 5-year survival rate of only 30% [24]. Hence, exploiting novel biomarkers and targets that could serve as early diagnosis tools and therapeutic targets for EOC is urgently needed. Our previous results suggested that the lncRNA CDKN2A-AS1 should be considered a sensitive and specific marker for EOC, as it was highly expressed in OC tissues when compared with that in normal ovarian tissue. KEGG pathway analysis showed that lncRNA CDKN2A-AS1 was involved in the BMP-SMAD signaling pathway, which participated in normal ovarian function [15,25]. SOSTDC1 (also known as WISE, USAG1, and ectodin) functions as an antagonist of BMPs [26]. Based on our knowledge, the expression and biological function of

SOSTDC1 in EOC remains unclear. In order to determine how SOSTDC1 and lncRNA CDKN2A-AS1 are implicated in EOC, we detected the expression level of CDKN2A-AS1 and SOSTDC1 in EOC tissues and cells (SKOV3 and OVCAR3), then studied the interaction and binding sites between CDKN2A-AS1 and SOSTDC1, determined the expression levels of key genes and proteins in EOC cells (SKOV3 and OVCAR3) and normal ovarian epithelial IOSE80 cells with overexpression and knockdown of the CDKN2A-AS1, examined cell proliferation, migration, and invasion, finally estimated the function of lncRNA CDKN2A-AS1 on the tumor growth by in vivo xenograft experiment.

The FISH and pull-down assay results validated that SOSTDC1 is a downstream target of CDKN2A-AS1. By directing binding with the
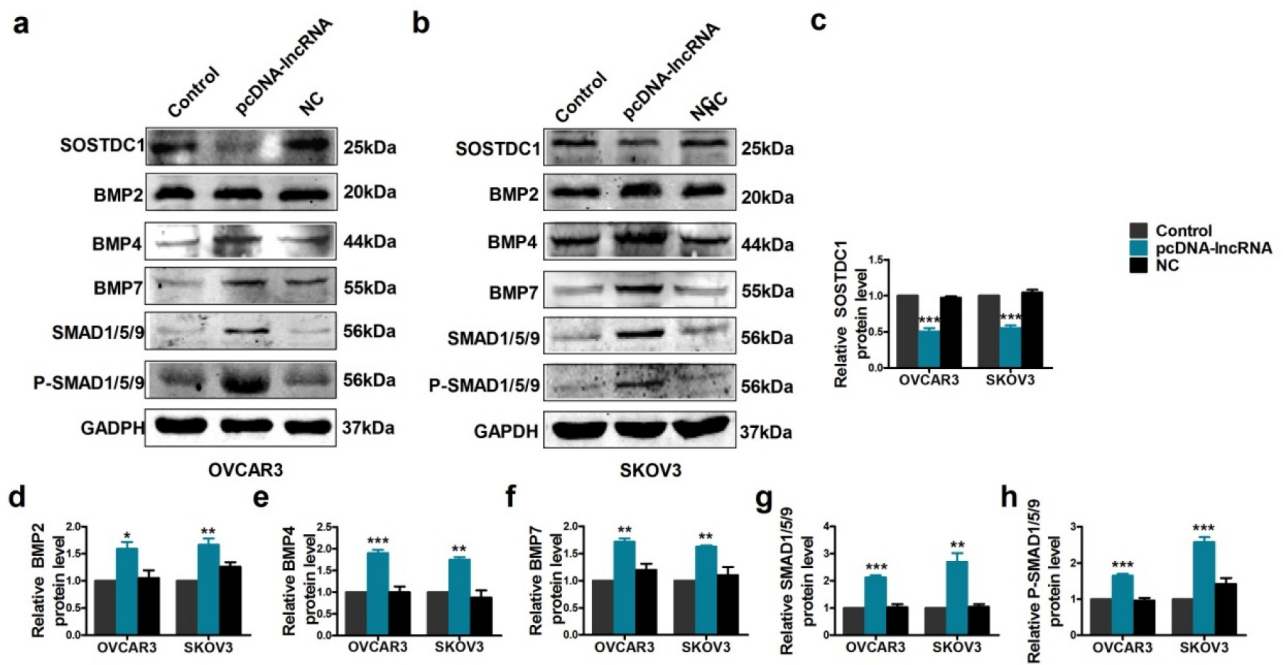
Figure 7. Effects of transfection of pcDNA CDKN2A-AS1 on the BMP-SMAD signaling pathway in SKOV3 and OVCAR3 cells. (a) Representative western blotting bands of proteins in OVCAR3 cells. (b) Representative western blotting bands of proteins in SKOV3 cells. Results of western blotting of SOSTDC1 (c), BMP2 (d), BMP4 (e), BMP7 (f), SMAD1/5/9 (g), and p-SMAD1/5/9 (h) in OVCAR3 cells and SKOV3 cells. *$p < 0.05$, **$p < 0.01$, ***$p < 0.001$ vs control.

SOSTDC1 gene, CDKN2A-AS1 downregulated the expression level of SOSTDC1, resulting in the activation of the BMP-SMAD signaling pathway. After transfection with the si-lncRNA of CDKN2A-AS1, the expression level of SOSTDC1 was elevated, while BMP2, BMP4, and BMP7 and the phosphorylation of SMAD1/5/9 were all suppressed. This phenomenon was reversed by transfection with the pc-DNA of CDKN2A-AS1. Western blotting assays further validated that high expression of CDKN2A-AS1 decreased the expression of SOSTDC1 and activated the BMP-SMAD signaling pathway.

Our results implied that CDKN2A-AS1 can function as a proto-oncogene that induces the development and metastasis of tumors. We identified that the CDKN2A-AS1/SOSTDC1 axis was functionally connected with the phenotype of EOC at the cellular level. Immunofluorescence staining assays proved the inhibitory effect of CDKN2A-AS1 against the protein output of SOSTDC1. Knockdown of CDKN2A-AS1 by siRNA inhibited metastasis and propagation of both SKOV3 and OVCAR3 cells. In contrast, diverse results were observed with pc-DNA of CDKN2A-AS1 treatment. In vivo xenograft showed that knockdown lncRNA CDKN2A-AS1

(si-lncRNA group) indeed suppressed the ovarian tumor growth, while overexpression of lncRNA (lncRNA group) promoted the ovarian tumor growth. The present study demonstrated that CDKN2A-AS1 was a vital regulator of the activation of the BMP-SMAD signaling pathway and regulated the output of the signaling proteins BMP2, BMP4, and BMP7 through binding the gene SOSTDC1, implying that CDKN2A-AS1 can be used as a novel diagnostic marker/a potential therapeutic target for EOC. However, several limitations of the present study existed, including the absence of an in vivo experiment regarding CDKN2A-AS1 in OC metastasis and the incomplete clinical data of the samples, in particular, the absence of lncRNA associated with differentiation, TNM stage, and lymph node metastasis. Additional experiments are required to further confirm the molecular mechanism of the binding of SOSTDC1 and CDKN2A-AS1. Furthermore, the regulatory mechanism of the CDKN2A-AS1/SOSTDC1 axis in other biological functions of ovarian cells remains to be investigated in future studies.

In conclusion, we validated the dysregulation of both the lncRNA CDKN2A-AS1 and the mRNA gene SOSTDC1 in EOC. The former was
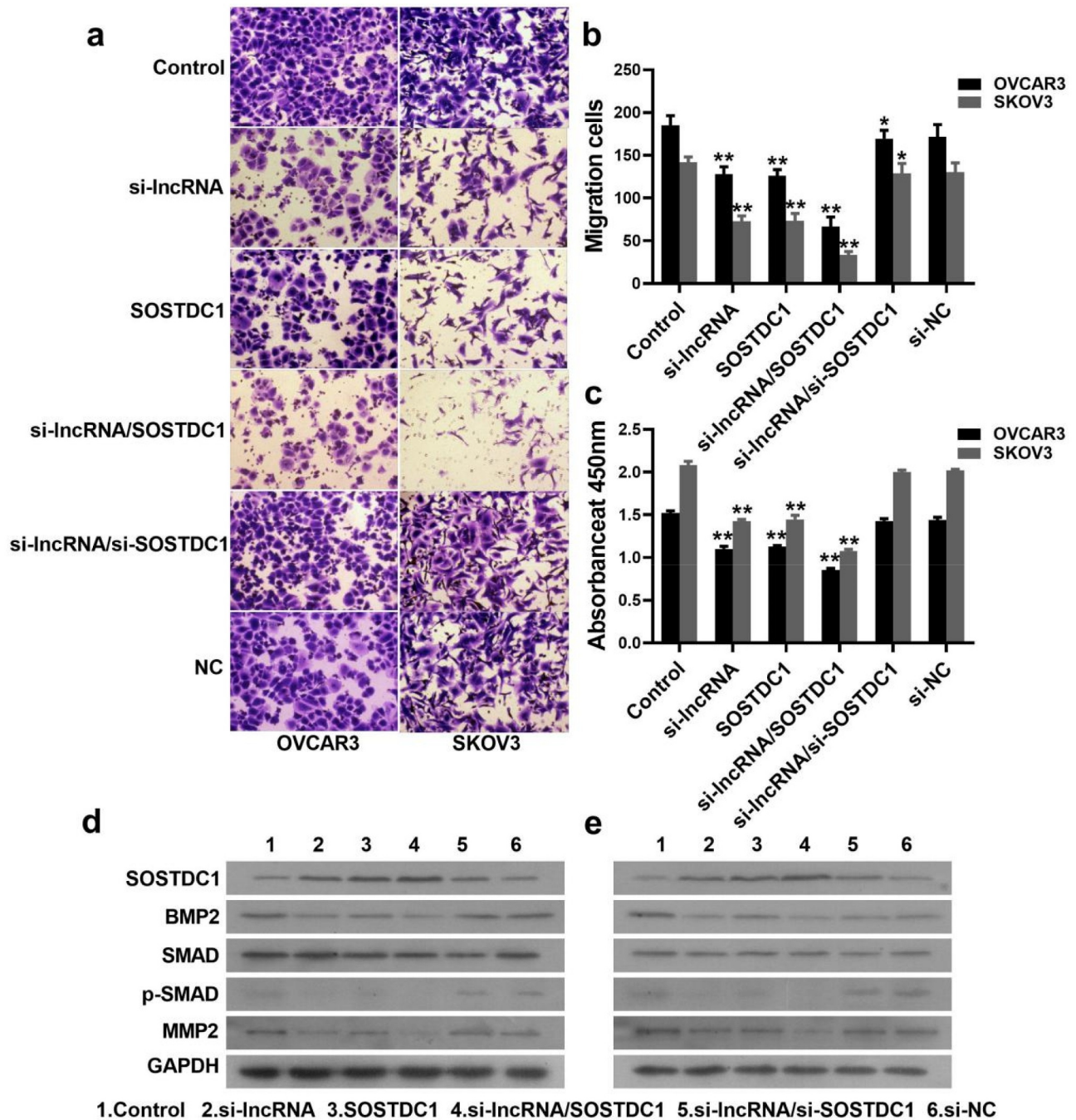
Figure 8. Effect of the SOSTDC1 and CDKN2A-AS1 on the proliferation, migration and invasion of the OVCAR3 and SKOV3 cells. (a, b) Migration assay was performed in OVCAR3 and SKOV3 cells. (c) The proliferation of the OVCAR3 and SKOV3 cells. (d) The protein expression level of BMP2, SMAD, p-SMAD and MMP2 were detected by WB in SKOV3 cells. (e) The protein expression level of BMP2, SMAD, p-SMAD and MMP2 were detected by WB in OVCAR3 cells. $*p < 0.05, **p < 0.01$ vs control.

overexpressed, whereas the latter was downregulated in patients with EOC. Meanwhile, we also validated the regulatory relationship between CDKN2A-AS1 and SOSTDC1, which involved direct binding. Our study substantiated that CDKN2A-AS1 modulated the BMP-SMAD signaling pathway through SOSTDC1, thereby promoting the tumorigenesis and progression of EOC. Our study not only contributed to the intensive study on the explicit mechanism of CDKN2A-AS1/SOSTDC1 but also provided promising therapeutic targets for the treatment of EOC.
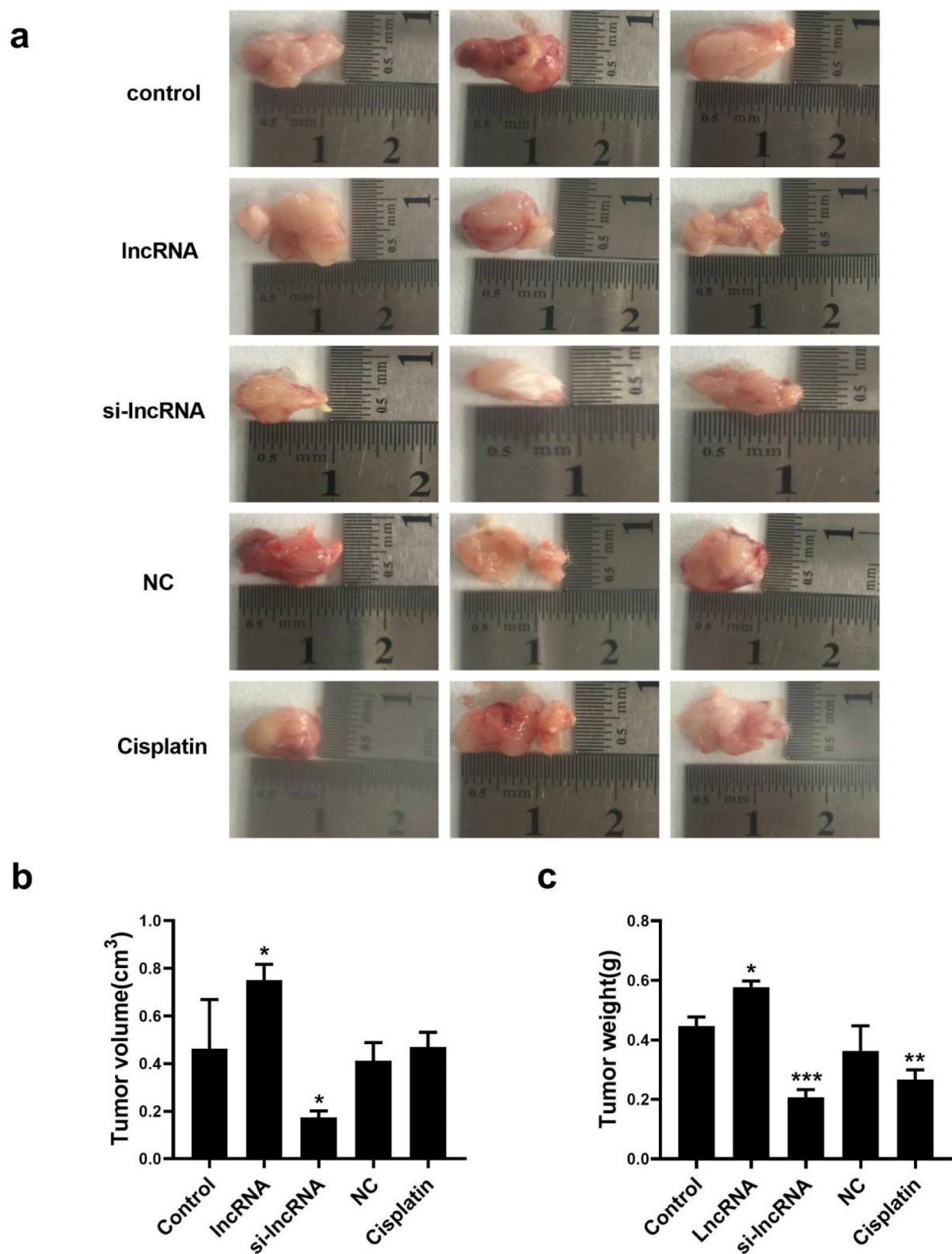
Figure 9. lncRNA CDKN2A-AS1 promoted tumor growth in the nude mouse xenograft tumor formation assay. (a) OVCAR3 cells stably knockdown lncRNA, overexpressed lncRNA were subcutaneously injected into nude mice. (b, c) The volume and weight of xenograft tumors in five groups with different treatment. *$p < 0.05$, **$p < 0.01$ vs control.

Disclosure statement

No potential conflict of interest was reported by the authors.

Funding

Data availability

The analyzed data sets generated during the present study are available from the corresponding author on reasonable request.

References

[1] Jemal A, Bray F, Center MM, et al. Global cancer statistics. CA Cancer J Clin. 2011;61(2):69–90.

[2] Morgan RJ, Armstrong DK, Boston B, et al. Epithelial Ovarian cancer. J National Compr Cancer Network. 2011;9(1):82–113.

[3] Zuberi M, Khan I, Gandhi G, et al. The conglomeration of diagnostic, prognostic and therapeutic potential of serum miR-199a and its association with clinico-pathological features in epithelial ovarian cancer. Tumor Biol. 2016;37(8):11259–11266.

[4] Zuberi M, Khan I, Mir R, et al. Utility of Serum miR-125b as a diagnostic and prognostic indicator and its alliance with a panel of tumor suppressor genes in epithelial ovarian cancer. PLoS One. 2016;11(4):e0153902–e.

[5] Dong R, Liu X, Zhang Q, et al. miR-145 inhibits tumor growth and metastasis by targeting metadherin in high-grade serous ovarian carcinoma. Oncotarget. 2014;5(21):10816–10829.

[6] Yamamoto T, Saitoh N. Non-coding RNAs and chromatin domains. Curr Opin Cell Biol. 2019;58:26–33.

[7] Mercer TR, Dinger ME, Mattick JS. Long non-coding RNAs: insights into functions. Nat Rev Genet. 2009;10 (3):155–159.

[8] Shi X, Sun M, Liu H, et al. Long non-coding RNAs: a new frontier in the study of human diseases. Cancer Lett. 2013;339(2):159–166.

[9] Guo F, Jiao F, Song Z, et al. Regulation of MALAT1 expression by TDP43 controls the migration and invasion of non-small cell lung cancer cells in vitro. Biochem Biophys Res Commun. 2015;465(2):293–298.

[10] Chen T, Liu Z, Zeng W, et al. Down-regulation of long non-coding RNA HOTAIR sensitizes breast cancer to trastuzumab. Sci Rep. 2019;9(1):19881.

[11] Qiu JJ, Lin YY, Ding JX. Long non-coding RNA ANRIL predicts poor prognosis and promotes invasion/metastasis in serous ovarian cancer. Int J Oncol. 2015;46(6):2497–2505.

[12] Gao J, Liu M, Zou Y, et al. Long non-coding RNA growth arrest-specific transcript 5 is involved in ovarian cancer cell apoptosis through the mitochondria-mediated apoptosis pathway. Oncol Rep. 2015;34(6):3212–3221.

[13] Zhang Y, Dun Y, Zhou S, et al. LncRNA HOXD-AS1 promotes epithelial ovarian cancer cells proliferation and invasion by targeting miR-133a-3p and activating Wnt/beta-catenin signaling pathway. Biomed Pharmacothe. 2017;96:1216–1221.

[14] Gao C, Zhao D, Zhao Q, et al. Microarray profiling and co-expression network analysis of lncRNAs and mRNAs in ovarian cancer. Cell Death Discov. 2019;5:93.

[15] Shepherd TG, Nachtigal MW. Identification of a putative autocrine bone morphogenetic protein-signaling pathway in human ovarian surface epithelium and ovarian cancer cells. Endocrinology. 2003;144(8):3306–3314.

[16] Yoshioka S, King ML, Ran S, et al. WNT7A regulates tumor growth and progression in ovarian cancer through the WNT/beta-catenin pathway. Mol Cancer Res. 2012;10(3):469–482.

[17] Hover LD, Young CD, Bhola NE, et al. Small molecule inhibitor of the bone morphogenetic protein pathway DMH1 reduces ovarian cancer cell growth. Cancer Lett. 2015;368(1):79–87.

[18] Gopal G, Raja UM, Shirley S, et al. SOSTDC1 down-regulation of expression involves CpG methylation and is a potential prognostic marker in gastric cancer. Cancer Genet. 2013;206(5):174–182.

[19] Clausen KA, Blish KR, Birse CE, et al. SOSTDC1 differentially modulates Smad and beta-catenin activation and is down-regulated in breast cancer. Breast Cancer Res Treat. 2011;129(3):737–746.

[20] Zhou Q, Chen J, Feng J, et al. SOSTDC1 inhibits follicular thyroid cancer cell proliferation, migration, and EMT via suppressing PI3K/Akt and MAPK/Erk signaling pathways. Mol Cell Biochem. 2017;435 (1–2):87–95.

[21] Faraahi Z, Baud'huin M, Croucher PI, et al. Sostdc1: a soluble BMP and Wnt antagonist that is induced by the interaction between myeloma cells and osteoblast lineage cells. Bone. 2019;122:82–92.

[22] Yanagita M, Oka M, Watabe T, et al. USAG-1: a bone morphogenetic protein antagonist abundantly expressed in the kidney. Biochem Biophys Res Commun. 2004;316 (2):490–500.

[23] Rawat A, Gopisetty G, Thangarajan R. E4BP4 is a repressor of epigenetically regulated SOSTDC1 expression in breast cancer cells. Cell Oncol. 2014;37(6):409–419.

[24] Noone AMHN, Krapcho M, Miller D, et al., eds. SEER cancer statistics review. MD: National Cancer Institute Bethesda; 2018. p. 1975–2015.

[25] Le Page C, Ouellet V, Madore J, et al. Gene expression profiling of primary cultures of ovarian epithelial cells identifies novel molecular classifiers of ovarian cancer. Br J Cancer. 2006;94(3):436–445.

[26] Lintern KB, Guidato S, Rowe A, et al. Characterization of wise protein and its molecular mechanism to interact with both Wnt and BMP signals. J Biol Chem. 2009;284(34):23159–23168.